Talanta 160 (2016) 367–374

Contents lists available at ScienceDirect

Talanta

journal homepage: www.elsevier.com/locate/talanta

Graphene oxide based electrochemical label free immunosensor for rapid and highly sensitive determination of tumor marker HSP70

Burcu Özcan*, Mustafa Kemal Sezgintürk

Namık Kemal University, Faculty of Science, Chemistry Department, Biochemistry Division, Tekirdağ, Turkey

ARTICLE INFO

Article history:
Received 21 March 2016
Received in revised form
10 July 2016
Accepted 20 July 2016
Available online 21 July 2016

Keywords:
Graphene oxide
HSP70
Cyclic voltammetry (CV)
Electrochemical impedance spectroscopy (EIS)
Label free immunosensor

ABSTRACT

In this study, it is aimed to design a label free immunosensor for determination of HSP70 (heat shock protein 70). Glassy carbon electrode was used as a working electrode. Graphene oxide was covered on the working electrode surface. AntiHSP70 as a biorecognition element of the biosensor was covalently immobilized onto the graphene oxide layer by using EDC/NHS chemistry. The immobilization of antiHSP70 and binding of HSP70 protein onto the electrode surface were monitored by cyclic voltammetry and electrochemical impedance spectroscopy. Single frequency technique was also utilized to monitor binding characterization of HSP70 and antiHSP70. Surface morphology was defined by using scanning electron microscopy. All important fabrication steps of the biosensor were optimized to prepare an ultrasensitive biosensor. Under optimum conditions, analytical studies such as linearity, repeatability, and reproducibility were also experienced. A linear detection range of HSP70 was determined between 12 and 144 fg/mL. Moreover, Kramer's Kronig transform was applied on impedance data. Finally, the biosensor was applied with real human blood serum samples and hopeful results were obtained.

1. Introduction

Chaperons or heat shock proteins (HSPs) are first identified in cells which exposed to heat shock [1,2]. Synthesis of HSPs increases under stress conditions such as high temperature, hypoxia, oxidative stress, pH, heavy metals and others [3,4]. They have an important role of cell differentiations [5]. In cancer cells, chaperones play a significant role in ordering transcription factors in protein kinases and the pathway of cell growth [6]. One of the most important members of HSP familly is HSP70 [7,8]. HSP70s exist in all alive organisms [9]. HSP70 is one of the chaperons that can directly contact to the ribosome [10]. HSP70 takes place in the cytoplasm [11]. One of the other functions of HSP70 is folding and preventing protein aggregation [12,13]. Under stress conditions, its synthesis starts and HSP70 releases in cytosol [14,15]. During the folding HSP70 uses ATPase and cofactors [16]. Increase in HSP70 synthesis informs about increased tumor cells [17,18]. On the other hand decrease in HSP70 synthesis informs about apoptosis [19].

Electrochemical impedance spectroscopy (EIS) is a very significant technique that is widely used in different area of surface investigations [20]. EIS is also an efficient method that is used to analyze complex electrical resistances, surface sensitivity and changes in amounts of systems [21–24]. This technique is often used to determine characterization and optimization of charge transfer through the membranes, membrane/solution interfaces and the surface modifications. Recently, this method has been preferred to monitor biosensor surfaces during the different fabrication processes and the specific interactions of biomolecules on the biosensing layers of the biosensors. Although the first examples of EIS usage in biosensor applications were reported at the end of 1980s, in recent years, there are many biosensor designs based on EIS method [25]. This method, differently from the conventional electrochemical techniques, can be used in any substance analysis and in interface processes in time constant changing from minutes to microseconds [26].

Glassy carbon electrode (GCE) has a lot of advantages such as large potential range, wide surface chemistry for electrochemical analyses, insignificant background current, low cost and usefulness for sensing and biosensing applications [27]. And so, electron transfer rate at glassy carbon electrode is usually slower than on splendid metal electrodes [28]. Concordantly, the electrochemical activity on glassy carbon electrodes can be enhanced toward certain analytes once their surfaces are peaked to an anodic oxidation because novel oxidized functional groups are generated after this method [29].

In the present study, a biosensor based on graphene oxide was developed by using EIS. Single frequency impedance was carried out to elicit binding characteristics between HSP70 and anti HSP70. In electrochemistry, there are a lot of techniques such as scanning electrochemical microscopy and scanning tunneling

* Corresponding author.
E-mail address: burcuozcannku@gmail.com (B. Özcan).

http://dx.doi.org/10.1016/j.talanta.2016.07.039
0039-9140/

microscopy to find out surfaces of electrodes. On the other hand, these methods take a long time and they are expensive. Furthermore, scanning electron microscope (SEM) can be utilized for surface characterization of the biosensors [30].

The purpose of this study is to design a biosensor for the determination of heat shock protein 70. The modification of the glassy carbon electrode with graphene oxide is highlighted in the present study. Anti-HSP70 was covalently immobilized onto the electrode surface covered with graphene oxide by using 1-ethyl-3-(3-dimethylaminopropyl) carbodiimide (EDC) and N-hydroxysuccinimide (NHS). Most importantly, the designed biosensor could make possible the determination of HSP70 as low as subfemtogram scales.

2. Experimental

2.1. Apparatus and instruments

All chemicals used in this research were purchased from Sigma- Aldrich (St. Louis, MO, USA). High surface area reduced graphene oxide was purchased from Graphene Supermarket Company. Black graphene oxide has 833 m^2/g surface area and its solid content is 98%. Average flake thickness and average particle size are 1 monolayer and ~3–5 μm, respectively. The dilution processes for HSP70 and antiHSP70 were realized with 50 mM phosphate buffer (pH 7.0). HSP70 and antiHSP70 were made at definite concentrations and kept at −20 °C. Glassy carbon electrode, 3 M Ag/ AgCl saturated with KCl and 10 mm-long platin wire were used as a working electrode, a reference electrode and a counter electrode, respectively. All electrodes were obtained from IBAS, Warwickshire, UK. The measurements were monitored by using Gamry Potentiostat/Galvanostat, Reference 1000 (Gamry Instruments, Warminster, USA) connected with a computer including Echem Analyst. Scanning electron microscopy (FEI-Quanta FEG 250 model) at the Scientific and Technological Research Center of Namık Kemal University (NABILTEM) was used to monitor the obtained changes on the electrode surface.

2.2. Preparation of graphene oxide solution

0.2 mg graphene oxide was weighed. Later 100 μl ultra-pure water was added over it. It was sonicated during an hour. After sonication, 0.024 g NaOH and 0.02 g trichloroacetic acid were added in this solution. The sonication process was repeated. Then 1 mL of ultra-pure water was added to the solution again. Lastly pH adjustment of this solution was done (pH=7).

2.3. Electrochemical characterization

EIS, CV and chronoimpedimetry were utilized to characterize the immobilization processes used in the biosensor. Potential range for CV was chosen between −0.5 and 1 V. (Step size: 20 mV, scan speed: 50 mV/s). The measurements were taken in 5 mM $K_3[Fe(CN)_6]/K_4[Fe(CN)_6]$ (1:1) solution including 0.1 M KCl. For taking electrochemical impedance measurements, 10 mV alternative current was performed to the surface of the electrode. The same redox probe was used in the EIS measurements. Impedance spectra were collected between 10.000 and 0.05 Hz. In the chronoimpedimetry measurements, a fixed potential was chosen as 0.01 V and the frequency was chosen 20 Hz. These measurements were performed in pH 7.0, 50 mM phosphate buffer.

2.4. Modification of the glassy carbon electrodes by graphene oxide

Firstly the glassy carbon electrodes were cleaned. In the cleaning procedure, the electrodes were given a polish with 0.05 μm aluminum oxide and then washed with ultra-pure water. Later, the electrodes were sonicated with HNO_3/pure acetone (1/1, v/v) solution for 3 min. After sonication, the electrodes were washed with ultra-pure water and dried by pure argon gas. After this procedure, graphene oxide solution was covered on the bare GCE surface and the electrodes were incubated for 30 min. Graphene oxide layer on the electrode surface makes possible the preparation of a cheap label free immunosensor for HSP70 biomarker.

2.5. Covalent attachment of antiHSP70 on graphene oxide modified electrodes

EDC/NHS was used for antiHSP70 immobilization. EDC was utilized as a crosslinking agent. NHS (N-hydroxysuccinimide) was utilized with EDC to increase the stability of the active ester. Glassy carbon electrodes treated with graphene oxide were plunged into a light-tight glass bottle including EDC/NHS couple (0.4 mM EDC, 0.1 mM NHS) for an hour in a dark medium. Then, glassy carbon electrodes were washed with ultra-pure water carefully and then dried by pure argon gas. Lastly, 5 μl of antiHSP70 solution was pipetted onto the electrode surface by a micropipette. After incubation with antiHSP70 for an hour in a humid ambient, the electrode was washed with ultra-pure water to remove physically adsorbed anti HSP70 molecules. Bare GCE and the modified electrodes were described as GCE, GCE/graphene oxide, GCE/graphene oxide/EDC-NHS, GCE/graphene oxide/EDC-NHS/antiHSP70, GCE/grapheneoxide/EDC-NHS/antiHSP70/BSA, GCE/graphene oxide/EDC-NHS/antiHSP70/BSA/HSP70.

3. Results and discussion

3.1. Immobilization steps of the designed biosensor

All immobilization steps in this study and binding of HSP70 onto the glassy carbon electrode surface were examined by using cyclic voltammetry (CV) and Electrochemical Impedance Spectroscopy (EIS). Whole processes were realized in $K_3[Fe(CN)_6]/K_4[Fe(CN)_6]$ as a redox probe. $K_3[Fe(CN)_6]/K_4[Fe(CN)_6]$ solution provides easy electron transport over the electroactive species on the electrode surface. EIS spectra and CV voltammograms belonging to the immobilization steps and developed equivalent circuit was shown in Fig. 1.

Electrochemical impedance spectroscopy technique could be shown by two commonly used methods: Nyquist and Bode plots [31]. The Nyquist diagrams of EIS spectra belonging to different layers of modified electrode were shown in Fig. 1A. Each impedance spectrum has a semicircle and a linear part. The semicircle parts at high frequencies hinge upon electron transfer process of $Fe(CN)_6^{3-/4-}$ and linear parts hinge upon diffusion. Charge transfer resistance on the electrode surface can be measured by using the diameter of semicircle. As can be seen in Fig. 1, an equivalent circuit can be modeled for measured EIS data. This equivalent circuit model includes ohmic resistance (Rs) related to the resistance of electrolyte solution between glassy carbon electrode and reference electrode, charge transfer resistance (Rct) and Warburg impedance (Zw). Rs and Zw are not influenced from immobilization processes of HSP70 biosensor but Rct influences from dielectric properties in the electrode/electrolyte interface [31]. This effect can be seen in Rct values measured from impedance spectra in Fig. 1A. Rct values increased owing to the fact that electrode surface became insulator in each immobilization step. These values belonging to covering of graphene oxide onto the surface, EDC/NHS activation, antiHSP70 immobilization and BSA treatment were measured as 206.6 Ω, 424.6 Ω, 1367 Ω and

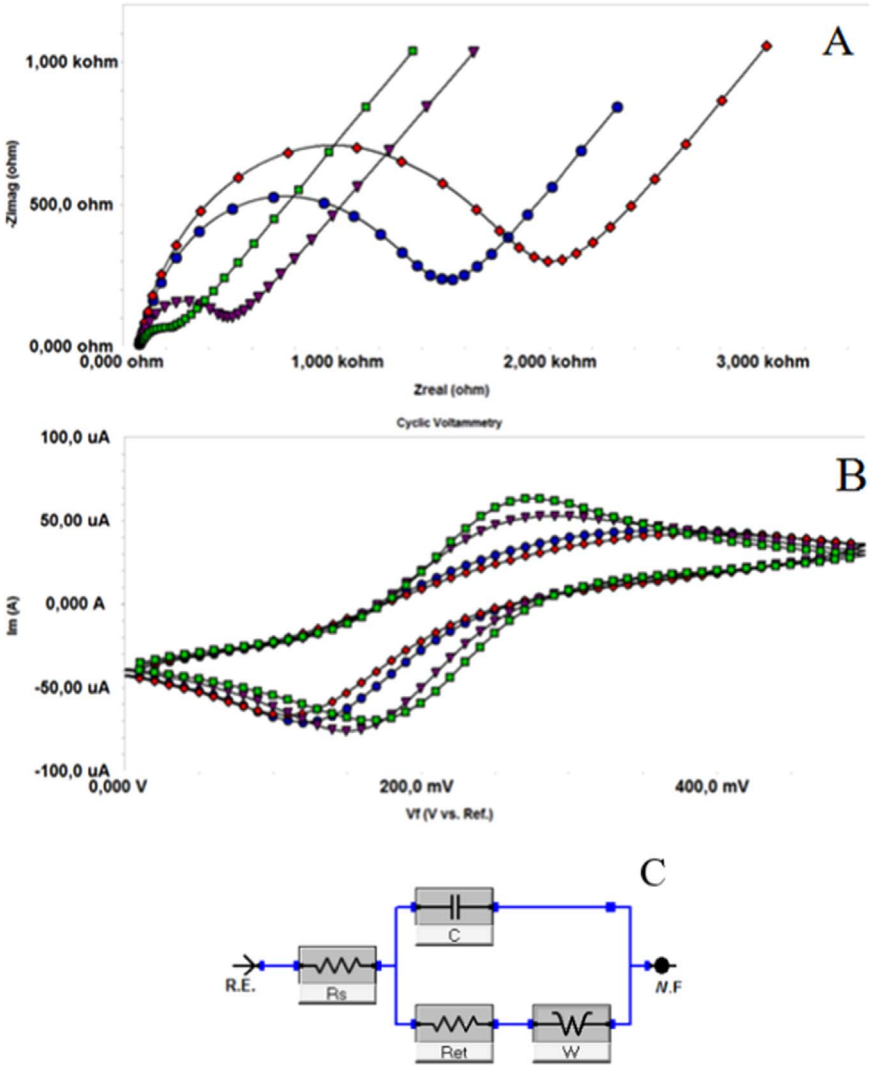

Fig. 1. A) EIS spectra and B) CV voltammogram belonging to the immobilization step of biosensor green (-■-■-): GCE/Graphene oxide, purple (-▾-▾): GCE/Graphene oxide/EDC- NHS, blue (-●-●-): GCE/Graphene oxide/EDC-NHS/AntiHSP70, red (-◆-◆-):GCE/Graphene oxide/EDC-NHS/AntiHSP70/BSA C) Equivalent circuit model applied to fit the impedance measurements. (For interpretation of the references to color in this figure legend, the reader is referred to the web version of this article.)

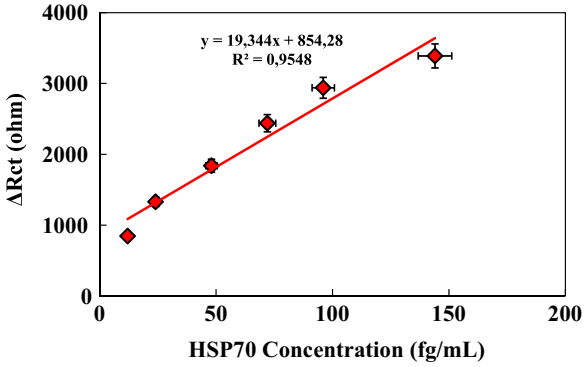

Fig. 2. Calibration curve of the antiHSP70 based biosensor (Calibration curve has been done with standard deviation for at list n=9 replicates.).

1840 Ω, respectively.

In this study, firstly graphene oxide was used as an immobilization supporting material. Graphene oxide gets attention by chemists and physicists under favor of its properties such as rapid electron transfer and biocompatibility. Thus, this material can be used in biosensors such as electrochemical, impedimetric, fluorescence biosensors and immunosensors. Graphene oxide has wider surface area in comparison to nanomaterials such as carbon nanotubes [32]. In this step of the study, the electrode surface was covered with graphene oxide and thus COO^- ends were generated on the surface. The diffusion of redox probe to the electrode surface became difficult because of the fact that COO^- functional groups of the graphene oxide were negatively charged. So, electron transfer resistance increased in comparison to bare electrode. To activate the COO- ends, EDC/NHS couple was used. EDC/NHS reaction includes the formation of active ester intermediate that is condensation product of carboxyl groups and NHS. This intermediate exhibits an excellent electrochemical activity [33]. COO- groups of graphene oxide could directly be activated with amine groups of EDC. However, NHS was also used with EDC to form more stable intermediate. The active COO- ends of graphene oxide interacted with amine groups of antiHSP70. And thus, antiHSP70 was covalently immobilized onto the electrode surface covered with graphene oxide. AntiHSP70 formed an insulator layer by generating a barrier effect on the surface. Thus, electron transfer resistance increased. When the biological components cannot be completely immobilized onto the surface, BSA can be used as a blocking agent [34]. The electrode surface was treated with BSA to block free active ends on the surface after immobilization of antiHSP70. In consequence of BSA treating, the charge transfer

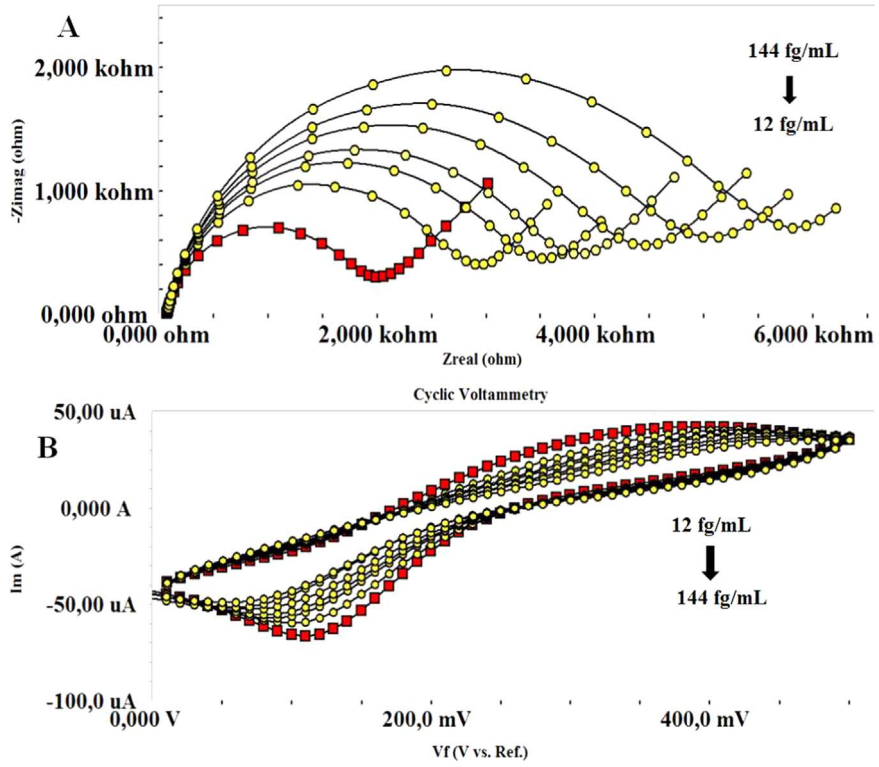

Fig. 3. EIS (A) and CV (B) results that were gotten for different HSP70 concentration.

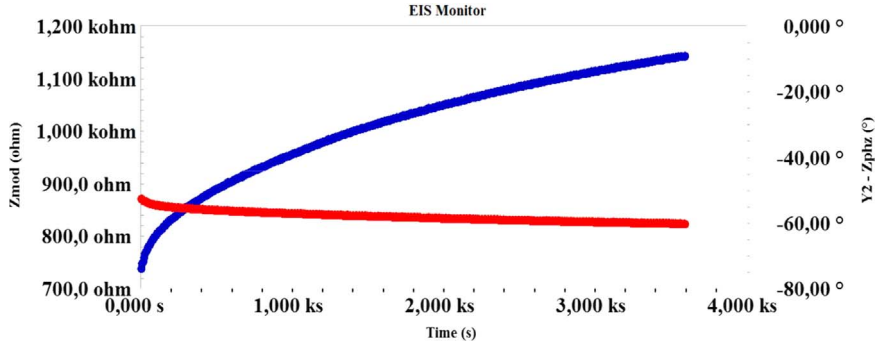

Fig. 4. The impedance of the designed biosensor based on antiHSP70 at fixed frequency.

resistance increased more and more. This can be seen in Fig. 1A.

Cyclic voltammetry technique was also used to support the data obtained from the impedance spectra. Thus, electrochemical behavior of the product formed by electrochemical reaction could be examined with anti-cycle. Cyclic voltammetry is an efficient technique to investigate the electron transfer rate of the modified electrodes. As is known, the change of oxidation and reduction peak currents in the cyclic voltammograms belonging to the different surfaces of electrodes can be based upon electron transfer rate and charge transfer resistance. When the Fig. 1B was examined, it could be seen that cyclic voltammetry voltammograms were in harmony with the impedance spectra. It was detected that the difference of the anodic and cathodic peak currents decreased because of the insulator layer when the electrode surface was covered with graphene oxide. This could be explained with the difficulty of diffusion of redox probes onto the electrode surface as such in the impedance spectra. After the COO- groups of graphene oxide were activated with EDC/NHS couple, the electron transfer onto the surface became more difficult and in consequence of this, the peak current differences decreased further. AntiHSP70 was immobilized onto the surface, the peak current differences decreased more and more because of the barrier effect of antiHSP70 immobilization. The last step of immobilization was the treatment with BSA. The anodic and cathodic peak current differences decreased more. BSA generated an extra insulator protein layer on the working electrode surface.

Immobilization process of the designed biosensor was seemed in Fig. 1S, Supplementary material.

3.2. Optimization studies of biosensor

Optimization steps are very important and necessary to construct a good, stable, repeatable, and reproducible biosensor. For this purpose all parameters such as graphene oxide amount, antiHSP70 concentration, antiHSP70 incubation time, and HSP70 incubation time were optimized.

Covering of the electrode surface with graphene oxide was the most important step for immobilizing of antiHSP70 onto the glassy carbon electrode surface. For that purpose, firstly different graphene oxide amounts such as 0.1 mg, 0.2 mg, 0.4 mg and 0.8 mg were studied for biosensor construction to determine how the graphene oxide amounts affect the biosensor performance. Rct

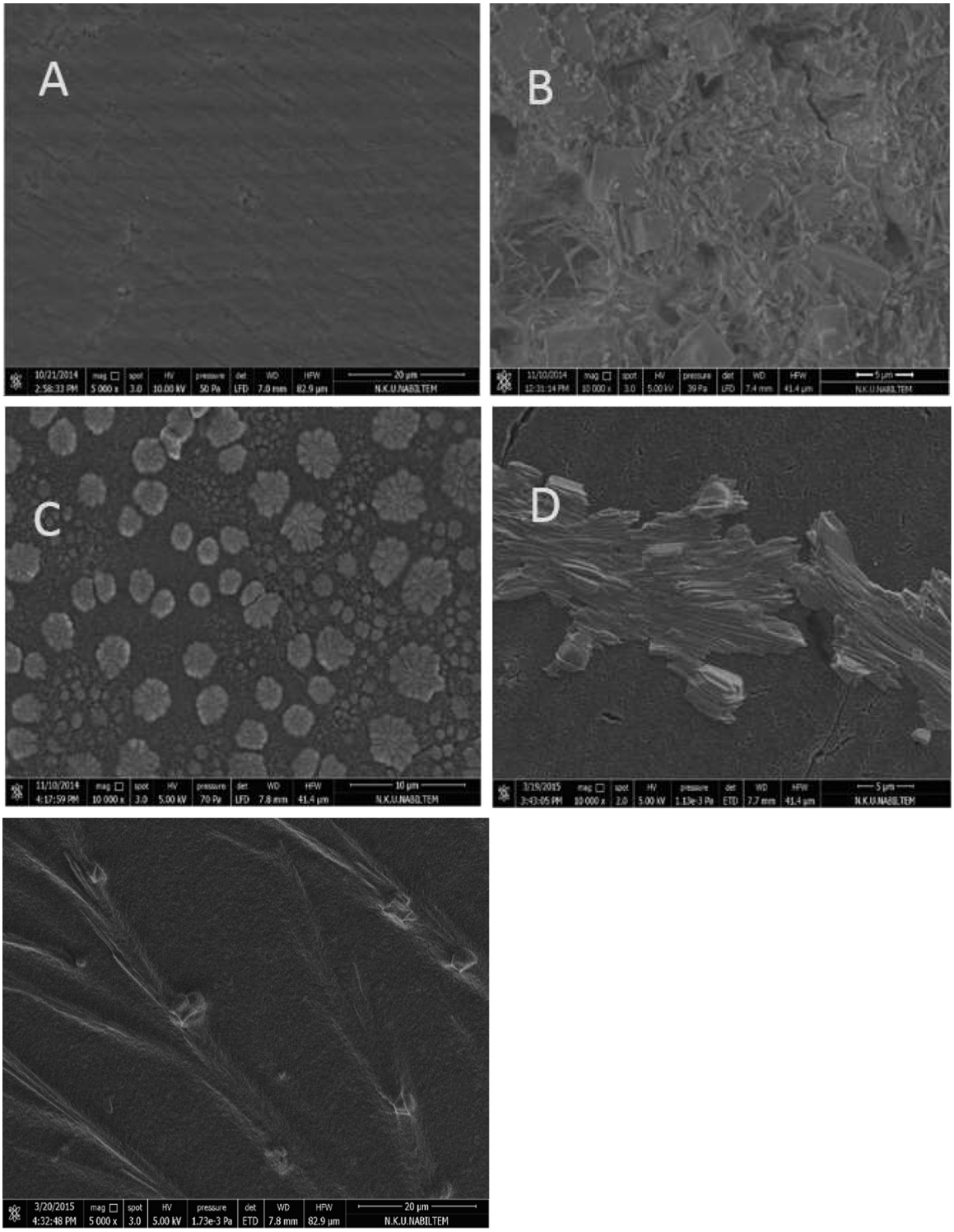

Fig. 5. SEM characterization of designed biosensor surfaces A) bare GCE B)GCE/Graphene oxide C) GCE/Graphene oxide/ antiHSP70 D)GCE/Graphene oxide/antiHSP70/BSA E) GCE/Graphene oxide/antiHSP70/BSA/HSP70.

values were calculated from the electrochemical impedance spectroscopy spectra of the biosensors prepared by using different graphene oxide amounts. The Rct values obtained from electrochemical impedance spectra were 892 Ω, 3400 Ω, 3610 Ω and 2340 Ω, correspondingly. When the Rct values obtained from EIS spectra were plotted versus the HSP70 concentrations, it was seemed that the signal of the biosensor increased by increasing of graphene oxide amounts. However, high amounts of graphene oxide such as 0.8 mg couldn't allow generating a stable covering. The signals of the biosensor prepared by using 0.2 mg graphene oxide were similar with the signals of the biosensor prepared by using 0.4 mg graphene oxide. When the amounts of graphene oxide used in this step were considered, 0.2 mg graphene oxide was chosen as optimum graphene oxide amount. And also, when 0.2 mg graphene oxide was used, it was seemed that antiHSP70 could perfectly immobilize onto the electrode surface more than when the other graphene oxide amounts were used. The highest signal was obtained when 0.2 mg graphene oxide was used. The

Table 1
The results of Kramer's Kronig transforms, sample analysis and comparison of used methods to determine HSP70.

The surface of biosensor			**Goodness of fit values**		
Kramer's–Kronig transforms for different layers of the antiHSP70 based biosensor GCE			1,448		
GCE/graphene oxide			6,402		
GCE/graphene oxide/EDC-NHS			2,699		
GCE/graphene oxide/anti-HSP70			2,700		
GCE/graphene oxide/anti-HSP70/BSA			13,94		
GCE/graphene oxide/anti-HSP70/BSA/HSP70			20,29		
HSP70 (fg/mL)					
HSP70 detection in artificial serum samples (fg/mL HSP70)					
Added	Found by the biosensor		Recovery (%)		Difference (%)
48	46.5		96.9		3.1
Analysis of real human serum sample (fg/mL HSP70)					
Serum	Found by the biosensor	Added HSP70	Totally found	Difference (%)	Relative difference (%)
1	40.4	48	90.6	102.5	2.5
Comparison of methods used to determine HSP70					
Methods	Measurement		Detection range		References
ELISA	Commercial kit		2×10^5–12.5×10^6 fg/mL		[37]
ELISA	Commercial kit		7.8×10^5–5×10^7 fg/mL		[38]
SPR	Magnetic microbeads based SPR		3×10^8–3×10^{10} fg/mL		[39]
LSPR	Label free SPR		9.2×10^5–4×10^9 fg/mL		[40]
Piezoelectric sensor	Biomimetic peptides		4.2×10^{15}–1.4×10^{16} fg/mL		[41]
The proposed biosensor	EIS		12–144 fg/mL		

Table 2
Comparison of the results obtained by using ELISA and the proposed biosensor.

	ELISA test	**The proposed biosensor**	**Difference (%)**
Sample 1	6.171 ng/mL	6.338 ng/mL	2.7
Sample 2	1.257 ng/mL	1.246 ng/mL	0.88
Sample 3	16.114 ng/mL	17.33 ng/mL	7.55
Sample 4	15.257 ng/mL	16.055 ng/mL	5.23
Sample 5	0.629 ng/mL	0.631 ng/mL	0.318

calibration curves belonging to these amounts of graphene oxide were shown in Fig. 2S, Supplementary material.

The next optimization step was the determination of antiHSP70 concentration needed for binding HSP70. To prepare a sensitive biosensor, antiHSP70 concentration optimization is an extremely important step. For this purpose, the activated electrode surfaces were incubated with 20 μg/mL, 40 μg/mL, 60 μg/mL and 80 μg/mL antiHSP70 concentrations. The immobilization of antiHSP70 made a barrier effect on the electrode surface and generated a non-conductive layer. Consequently, charge transfer resistances increased with the increase in antiHSP70 amount. The results showed that biosensor performance were also dependent to the concentration of antiHSP70. The Rct values calculated by using electrochemical impedance spectra were 1250 Ω, 2600 Ω, 1970 Ω and 2160 Ω, respectively. When the HSP70 calibration graphs obtained by these experiments were evaluated, the signals obtained by using 40 μg/mL of antiHSP70 were higher than the signals obtained by using 20 μg/mL anti HSP70. Namely, an increase in the concentration of antiHSP70 induced an increase in the signal. However, more increase in the concentration of antiHSP70 did not affect the signal. It could be concluded from the results, the signals were very similar to each other obtained 60 μg/mL and 80 μg/mL of antiHSP70 were used. The best biosensor response was obtained with 40 μg/mL of antiHSP70. Finally, 40 μg/mL was chosen as the optimum antiHSP70 amount. HSP70 calibration curves obtained by this optimization step were shown in Fig. 3S, Supplementary material. Moreover, EIS and CV results belonging to the biosensor prepared with 40 μg/mL of antiHSP70 were also represented in Fig. 4S, Supplementary material.

After the optimization of antiHSP70 concentration, incubation time for antiHSP70 was determined for immobilizing of antibody antiHSP70 onto the electrode surface at a maximum efficiency. For this purpose, four different incubation times were studied to immobilize antiHSP70. These periods were 30, 45, 60, 75 min, respectively. Moreover, the Rct values obtained by EIS spectra were 1020 Ω, 875 Ω, 1300 Ω and 1040 Ω, correspondingly. HSP70 calibration curves obtained by the biosensors fabricated by using different antiHSP70 incubation periods were shown in Fig. 5S, Supplementary material. In consequence of antiHSP70 incubation time optimization, it was not possible to immobilize antiHSP70 onto the electrode surface in short periods such as 30 min. In addition, the results showed that the electrode surface did not effectively formed after incubation for longer HSP70 incubation periods longer than 60 min such as 75 min. When antiHSP70 incubation period was chosen as 60 min, a sensitive and high performance biosensor could be obtained. As a conclusion, the incubation time of antiHSP70 immobilization was chosen as 60 min.

After all parameters were optimized, the binding of HSP70 onto the surface was examined. For this purpose, the electrodes were incubated with HSP70 for 30, 45, 60 and 75 min, respectively. Calibration curves belonging to these times were given in Fig. 6S, Supplementary material. The signals of biosensor increased with the increasing incubation time of HSP70. When 30 min and 45 min incubation times were utilized, the signals were close to each other. However when 60 min incubation time was used, it was seemed that the signals were significantly increased. It showed that 30 min and 45 min were inadequate for binding of HSP70 onto the surface. In longer time as 75 min, it was monitored that the capacity of HSP70 binding onto the surface decreased because of possible deformation of the surface. Consequently, the best results were obtained when the electrodes were incubated with HSP70 for 60 min. Namely, 60 min was chosen as the incubation time of HSP70.

3.3. Analytical studies of designed biosensor

In this study, under the optimum conditions, to determine linear range, repeatability, reproducibility of biosensor, analytical studies were also done.

Firstly, linear range of HSP70 was determined. In consequence of this step, the linear range of HSP70 was determined between 12 fg/mL and 144 fg/mL. HSP70 calibration curve was shown in Fig. 2. The electrochemical impedance spectra and cyclic voltammetry voltammograms belonging to increasing HSP70 concentrations were also showed in Fig. 3. In addition, one of the most important parameter to determine the sensitivity of designed biosensor was the limit of detection (LOD) and the limit of quantitation (LOQ) values. LOD means the lowest HSP70 amount that could be determined to be statistical by the biosensor. LOQ means the lower limit of quantitation. To calculate LOD and LOQ, following equations were used: $[k^*S_{blank}/m]$. In this equation, k is a constant, it is accepted as 3 in LOD calculations and as 10 in LOQ calculations. S_{blank} is the signal of blank sample and m is the slope [35]. LOD was found as 0.765 fg /mL. LOQ was found as 2.55 fg /mL.

Repeatability is an expression of the differences of results obtained from the measurements taken by using same device, same samples under the same conditions. In this respect, taking repeatable results is extremely important. This step acted as a significant role for the characterization of the biosensor. For this

purpose, 72 fg/mL standard HSP70 solution was utilized in the repeated measurements. In addition, by using the results of the EIS measurements, statistical parameters were calculated. The average value, standard deviation and coefficient of variation were found as 72.6 fg/mL ± 4.8 fg /mL and % 6.6, respectively.

One of the most important features expected from the designed biosensor is a perfect reproducibility. To use the biosensor in routine analyze, reliability and reproducibility of the biosensor is very important and a necessary parameter. For this reason under the optimum conditions, ten numbers of electrodes were prepared. Rct values obtained from the electrochemical impedance spectra were plotted versus HSP70 concentrations and were compared with each other. The results revealed that the curves were very similar to each other. It showed that this immobilization process could fabricate a reproducible biosensor successively. And also, relative standard deviation (RSD) values related to intercept and slope values of HSP70 calibration graphs obtained by the reproducibility experiments were calculated as % 0.96 and % 1.2.

After reproducibility study of the biosensor, to understand the interaction between antiHSP70 and HSP70, single frequency technique was used. This system based on impedance measurement at fixed frequency provides the evaluation of both the changes on the surface and kinetics parameters of interactions during the measurement simultaneously. The impedance measurements were taken versus time at a fixed frequency. These measurements were realized in pH 7 phosphate buffer. Accordingly, the changes of impedance could be controlled with repeat time and total time. For this reason, the measurement was taken at 20 Hz fixed frequency. This measurement continued for 60 min as a function of time and phase angle. In Fig. 4, the results of measurements at fixed frequency were shown. As seen in Fig. 4, the measurements could present information about the binding of HSP70 and antiHSP70. The blue curve shows the change of impedance as a function of time. The red curve shows the change of phase angle as a function of time. The changes of phase angle and charge transfer resistance results from the interaction between the HSP70 and antiHSP70.

Fig. 7S shows the Bode plot for the evaluation of the optimum frequency used in single frequency impedance. Bode plots procure the impedance data as a function of frequency and were analyzed carefully. As seen in Fig. 7S, an increase was monitored in the frequency range of 10–100 Hz. The working frequency was chosen as 20 Hz.

SEM (Scanning Electron Microscope) technique is an important tool to monitor the changes during the biosensor fabrication. The resulting SEM pictures are given in Fig. 5.

The changes that were monitored by SEM technique were agreed with the results obtained with the impedance characterization studies. Consequently, the accuracy of measurements could be proved and the changes in the surface could be monitored by using SEM technique.

The other important parameter for this study was Kramer's Kronig transform. It is used to determine whether the impedance spectra of the designed biosensor are affected from the deviation obtained because of external factors. The principle of Kramer's Kronig transform is based on calculation of reel part of impedance data by using imaginative part or calculation of imaginative part by using reel part. This method is extremely important to interpret and analyze the electrochemical impedance spectroscopy [35]. The plots of Kramer's Kronig transform were seemed in Fig. 8S, Supplementary material. The goodness of fit values for different biosensor surfaces were shown in Table 1.

There are many studies to detect HSP70 by using tests such as ELISA were reported. Enzyme-linked Immunosorbent Assays (ELISAs) combine the specificity of antibodies with the sensitivity of simple enzyme assays by using antibodies or antigens coupled to an easily-assayed enzyme. ELISAs can provide a useful measurement of antigen or antibody concentration. There are two main variations of this method; in the first one, the ELISA can be used to detect the presence of antigens that are recognized by an antibody and in the second one, it can be used to test for antibodies that recognize an antigen. However ELISA system is time-consuming and expensive [36]. Cui and workers found HSP70 detection range as 0.2–12.5 ng/mL. They used ELISA method for the detection of HSP70 concentration [37]. Zhu and workers determined HSP70 protein levels using commercially available ELISA kits. The standard curve has a range of 0.78–50 ng/mL [38]. However, the studies of HSP70 determination by using biosensors are less than ELISA tests. Sun and workers determined the detection range of HSP70 as 0.3–30.0 μg/mL by using surface plasmon resonance (SPR) based tecniques [39]. In the proposed study, HSP70 at lower concentrations could be determined more effectively in comparison to these studies discussed. Label free immunosensors are cheaper and easier than SPR based tecniques. The comparison of developed methods to determine HSP70 was shown in Table 1. The proposed biosensor was applied to the artificial serum samples and real human serum. The results were also shown in Table 1. It is remarkable that designed biosensor could be applied to both artificial serum samples and real human serum samples. In addition, the proposed biosensor has been compared with a commercial ELISA technique for the same human serum samples. The detection range of HSP70 for this commercial kit is in the range of 0.312–20 ng/mL. The comparison of these two tecniques has been shown in Table 2. Finally, one sample *t* test was used to demonstrate either both methods provide the same information. The differences between the values found after these analyses were not statistically meaningful because $p=0.08$ value found with *t* test were higher than 0.05. As a conclusion, the results of these two methods were really consistent.

4. Conclusion

In this study, we report a design of a simple and a high performance biosensor to determine HSP70 in real human serum samples. For this purpose, the electrode surface was treated with graphene oxide firstly. Graphene oxide has a lot of advantages such as wide surface area, rapid electron transport and biocompatibility. Thanks to these properties, it can be widely used in biosensors such as immunosensors, electrochemical sensors and fluorescence sensors. All parameters were optimized to obtain a good biosensor response. In addition, it could be seen that the impedance of biosensor was stable and linear by using Kramer's-Kronig transforms. A linear range of HSP70 was determined as 12–144 fg /mL. Single frequency technique was also used for determining the binding characteristics of antiHSP70 and HSP70. This biosensor has a good repeatability and reproducibility. Finally the real human serum sample analyses were performed by the proposed biosensor and a commercial ELISA kit, and the results were perfectly agreed with the each other.

Acknowledgment

This work was funded by TÜBİTAK (The Scientific and Technological Research Council of Turkey, (Project number: 113 Z 678), this assistance is greatly acknowledged.

Appendix A. Supplementary material

Supplementary data associated with this article can be found in the online version at http://dx.doi.org/10.1016/j.talanta.2016.07.039.

References

[1] M.E. Feder, G.E. Hofmann, Heat-shock proteins, molecular chaperones, and the stress response: Evolutionary and ecological physiology, Annu. Rev. Physiol. 61 (1999) 243–282.
[2] C. Georgopoulos, W.J. Welch, Role of the major heat shock proteins as molecular chaperones, Annu. Rev. Cell Biol. 9 (1993) 601–634.
[3] M.P. Mayer, B. Bukau, Hsp70 chaperones: cellular functions and molecular mechanism, Cell. Mol. Life Sci. 62 (2005) 670–684.
[4] J.P. Hendrick, F.U. Hartl, Molecular chaperone functions of heat-shock proteins, Annu. Rev. Biochem. 62 (1993) 349–384.
[5] E. Pyza, P. Mak, P. Kramarz, R. Laskowski, Heat shock proteins (HSP70) as biomarkers in ecotoxicological studies, Ecotoxicol. Environ. Saf. 38 (1997) 244–251.
[6] M.E. Murphy, The HSP70 family and cancer, Carcinogenesis 34 (2013) 1181–1188.
[7] B. Bukau, A.L. Horwich, The Hsp70 and Hsp60 chaperone machines, Cell 92 (1998) 351–366.
[8] J.G. Kiang, G.C. Tsokos, Heat shock protein 70 kDa: molecular biology, biochemistry, and physiology, Pharmacol. Ther. 80 (1998) 183–201.
[9] D.R. Ciocca, S.K. Calderwood, Heat shock proteins in cancer: diagnostic, prognostic, predictive, and treatment implications, Cell Stress Chaperons 10 (2) (2005) 86–103.
[10] S. Takahashi, T. Mikami, Y. Watanabe, Correlation of heat shock protein 70 expression with estrogen receptor levels in invasive human breast cancer, Am. J. Clin. Pathol. 101 (1994) 519–525.
[11] M. Zylicz, A. Wawrzynow, Insights into the function of Hsp70 chaperones, IUBMB Life 51 (2001) 283–287.
[12] H.H. Kampinga, E.A. Craig, The HSP70 chaperone machinery: J proteins as drivers of functional specificity, Nat. Rev. Mol. Cell Biol. 11 (2010) 579–592.
[13] J. Frydman, Folding of newly translated proteins in vivo: the role of molecular chaperones, Annu. Rev. Biochem. 70 (2001) 603–647.
[14] I. Guzhova, K. Kislyakova, O. Moskaliova, I. Fridlanskaya, M. Tytell, M. Cheetham, B. Margulis, In vitro studies show that Hsp70 can be released by glia and that exogenous Hsp70 can enhance neuronal stress tolerance, Brain Res. 914 (2001) 66–73.
[15] M.J. Schlesinger, Heat shock proteins, J. Biol. Chem. 265 (1990) 12111–12114.
[16] X.B. Qiu, Y.M. Shao, S. Miao, L. Wang, The diversity of the DnaJ/Hsp40 family, the crucial partners for Hsp70 chaperones, Cell Mol. Life Sci. 63 (22) (2006) 2560–2570.
[17] C. Jolly, R.I. Morimoto, Role of the heat shock response and molecular chaperones in oncogenesis and cell death, J. Natl. Cancer Inst. 92 (2000) 1564–1572.
[18] M.G. Santoro, Heat shock factors and the control of the stress response, Biochem. Pharmacol. 59 (2000) 55–63.
[19] D.D. Mosser, A.W. Caron, L. Bourget, C. Denis- Larose, B. Massie, Role of the human heat shock protein hsp70 in protection against stress-induced apoptosis, Mol. Cell. Biol. 17 (1997) 5317–5327.
[20] C.C. Hu, C.H. Chu, Electrochemical impedance characterization of polyaniline-coated graphite electrodes for electrochemical capacitors—effects of film coverage/thickness and anions, J. Electroanal. Chem. 503 (2001) 105–116.
[21] E.B. Bahadır, M.K. Sezgintürk, Poly(amidoamine) (PAMAM): an emerging material for electrochemical bio(sensing) applications, Talanta 148 (2016) 427–438.
[22] M.N. Sonuç Karaboğa, Ç. Sayıklı Şimşek, M.K. Sezgintürk, AuNPs modified, disposable, ITO based biosensor: early diagnosis of heat shock protein 70, Biosens. Bioelectron. 84 (2016) 22–29.
[23] Ç. Sayıklı Şimşek, M.N. Sonuç Karaboğa, M.K. Sezgintürk, A new immobilization procedure for development of an electrochemical immunosensor for parathyroid hormone detection based on gold electrodes modified with 6-mercaptohexanol and silane, Talanta 144 (2015) 210–218.
[24] G. Yeşiller, M.K. Sezgintürk, A new methodology for the determination of enzyme activity based on carbon nanotubes and glucose oxidase, J. Pharm. Biomed. Anal. 115 (2015) 254–259.
[25] M.Ç. Canbaz, Ç. Sayıklı Şimşek, M.K. Sezgintürk, Electrochemical biosensor based on self-assembled monolayers modified with gold nanoparticles for detection of HER-3, Anal. Chim. Acta 814 (2014) 31–38.
[26] A.J. Bard, L.R. Faulkner, Electrochemical Methods: Fundamentals and Applications, 2nd ed., 2nd John Wiley and Sons Inc., New York, 2001.
[27] B. Uslu, S.A. Ozkan, Solid electrodes in electroanalytical chemistry: present applications and prospects for high throughput screening of drug compounds, Comb. Chem. High Throughput Screen. 10 (2007) 495–513.
[28] J. Wang, Electroanalytical Chemistry, 3rd ed., Wiley-VCH Pub, New Jersey 2006, p. 136.
[29] T. Atoguchi, A. Aramata, A. Kazusaka, M. Enyo, Electrocatalytic activity of Co^{II} TPP-pyridine complex modified carbon electrode for CO_2 reduction, J. Electroanal. Chem. Interfacial Electrochem. 318 (1991) 309–320.
[30] A.J. Bard, M.V. Mirkin, Scanning Electrochemical Microscopy, CRC Press, Boca Raton, Florida, 2012.
[31] B. Özcan, B. Demirbakan, G. Yeşiller, M.K. Sezgintürk, Introducing a new method for evaluation of the interaction between an antigen and an antibody: single frequency impedance analysis for biosensing systems, Talanta 125 (2014) 7–13.
[32] S. Alwarappan, S. Boyapalle, A. Kumar, C. Li, S. Mohapatra, Comparative study of single-, few-, and multilayered graphene toward enzyme conjugation and electrochemical response, J. Phys. Chem. C 116 (2012) 6556–6559.
[33] E. Asav, M.K. Sezgintürk, Comparative study of single-, few-, and multilayered graphene toward enzyme conjugation and electrochemical response, Int. J. Biol. Macromol. 66 (2014) 273–280.
[34] Q. Shi, X. Chen, T. Lu, X. Jing, The immobilization of proteins on biodegradable polymer fibers via click chemistry, Biomaterials 29 (2008) 1118–1126.
[35] M.N. Sonuç, M.K. Sezgintürk, Ultrasensitive electrochemical detection of cancer associated biomarker HER3 based on anti-HER3 biosensor, Talanta 120 (2014) 355–361.
[36] ⟨http://www.elisa-antibody.com/ELISA-Introduction/ELISA-Principle⟩.
[37] X. Cui, J. Xing, Y. Liu, Y. Zhou, X. Luo, Z. Zhang, W. Han, T. Wu, W. Chen, COPD and levels of Hsp70 (HSPA1A) and Hsp27 (HSPB1) in plasma and lymphocytes among coal workers: a case-control study, Cell Stress Chaperons 20 (3) (2015) 473–481.
[38] J. Zhu, A.A. Quyyumi, H. Wu, G. Csako, D. Rott, A. Zalles-Ganley, J. Ogunmakinwa, J. Halcox, S.E. Epstein, Increased serum levels of heat shock protein 70 are associated with low risk of coronary artery disease, Arterioscler. Thromb. Vasc. Biol. 23 (2003) 1055–1059.
[39] Y. Sun, Y. Bai, D. Song, X. Li, L. Wang, H. Zhang, Design and performances of immunoassay based on SPR biosensor with magnetic microbeads, Biosens. Bioelectron. 23 (4) (2007) 473–478.
[40] R. Denomme, A label- free Biosensor for Heat Shock Protein 70 Using Localized Surface Plasmon Resonance, 2012.
[41] M. Mascini, M. Del Garlo, D. Compagnone, I. Cozzani, P. Tiscar, C. Mpamhanga, B. Chen, Piezoelectric sensors based on biomimetic peptides for the detection of heat shock proteins (HSPs) in mussels, Anal. Lett. 39 (8) (2006) 1627–1642.